Journal of Coordination Chemistry
Publication details, including instructions for authors and subscription information:
http://www.tandfonline.com/loi/gcoo20

Coinage (Cu, Ag) metal derivatives of salicylaldehyde N-ethylthiosemicarbazone: synthesis, spectroscopy, and structures

Tarlok S. Lobana [a], Poonam Kumari [a], Ishveen Kaur [a], Nirandeep Kaur [a], Ginni Garg [a] & Ray J. Butcher [b]

[a] Department of Chemistry, Guru Nanak Dev University, Amritsar 143005, India

[b] Department of Chemistry, Howard University, Washington, DC 20059, USA

Published online: 23 Apr 2012.

To cite this article: Tarlok S. Lobana, Poonam Kumari, Ishveen Kaur, Nirandeep Kaur, Ginni Garg & Ray J. Butcher (2012) Coinage (Cu, Ag) metal derivatives of salicylaldehyde N-ethylthiosemicarbazone: synthesis, spectroscopy, and structures, Journal of Coordination Chemistry, 65:10, 1750-1764, DOI: 10.1080/00958972.2012.680211

To link to this article: http://dx.doi.org/10.1080/00958972.2012.680211

Journal of Coordination Chemistry
Vol. 65, No. 10, 20 May 2012, 1750–1764

Coinage (Cu, Ag) metal derivatives of salicylaldehyde N-ethylthiosemicarbazone: synthesis, spectroscopy, and structures

TARLOK S. LOBANA*†, POONAM KUMARI†, ISHVEEN KAUR†, NIRANDEEP KAUR†, GINNI GARG† and RAY J. BUTCHER‡

†Department of Chemistry, Guru Nanak Dev University, Amritsar 143005, India
‡Department of Chemistry, Howard University, Washington, DC 20059, USA

(*Received 20 December 2011; in final form 28 February 2012*)

Reactions of copper(I) halides with triphenyl phosphine in acetonitrile followed by the addition of salicylaldehyde N-ethylthiosemicarbazone {(2-OH–C_6H_4)(H)C^2=N^3–N^2H–C^1(=S)N^1HEt, H_2stsc-NEt} in chloroform in 1 : 2 : 1 (Cl) or 1 : 1 : 1 (Br, I) molar ratios yield mononuclear, [CuCl(η^1-S-H_2stsc-NHEt)(PPh_3)$_2$] (**1**) and sulfur-bridged dinuclear, [Cu_2X_2(μ-S-H_2stsc-NEt)$_2$(PPh_3)$_2$] (X = Br, **4**; I, **5**) complexes. Similarly, reaction of silver halides (Cl, Br) with H_2stsc-NEt in acetonitrile followed by the addition of PPh_3 to the solid that formed (1 : 1 : 2 molar ratio), yielding mononuclear complexes, [AgX(η^1-S-H_2stsc-NHEt)(PPh_3)$_2$] (Cl, **2**; Br, **3**). All these complexes are characterized with analytical data, IR, and NMR spectroscopy and single-crystal X-ray crystallography. The ligand favored η^1-S bonding in **1**, **2**, and **3**, and μ-S bonding in **4** and **5**. Cu···Cu contacts were 3.063 Å. The complexes form 1-D or 2-D H-bonded networks, entrapping solvent in some cases.

Keywords: Salicylaldehyde N-ethylthiosemicarbazone; Triphenyl phosphine; Copper; Silver; Sulfur bridging

1. Introduction

N, S-donor thiosemicarbazones, ($R^1R^2C^2$=N^3–N^2(H)–C(=S)$N^1R^3R^4$), have shown variable donor properties and structural diversity involving the formation of mono-, di-, and poly-nuclear complexes. In addition these thio-ligands and their complexes find catalytic, analytical, and biological applications [1–3]. Among transition metals, the thiosemicarbazone complexes of nickel(II) and copper(II) have been intensively studied, as some of them show anticancer, antifungal, and antibacterial activities [4–8]. Coordination chemistry of thiosemicarbazones with copper(I) and silver(I) halides have been reported [9–29], as not much was known earlier for these metals in their univalent state [1].

Benzaldehyde thiosemicarbazone (Hbtsc-NH_2: R^1, R^2 = H) with copper(I) halides (CuX) in the presence of PPh_3 as a co-ligand formed three types of complexes: type 1 for

*Corresponding author. Email: tarlokslobana@yahoo.co.in

ISSN 0095-8972 print/ISSN 1029-0389 online © 2012 Taylor & Francis
http://dx.doi.org/10.1080/00958972.2012.680211

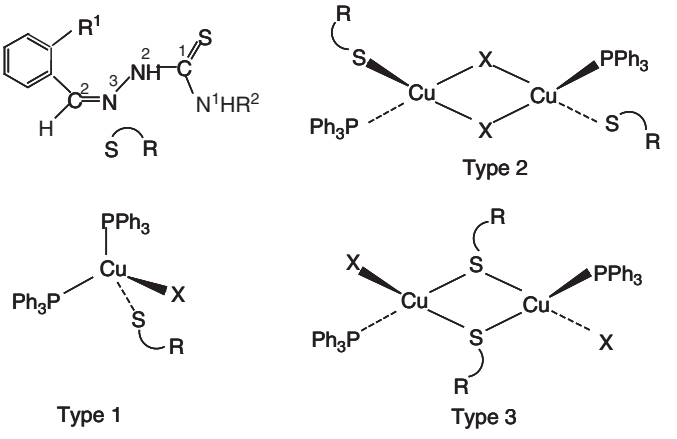

Scheme 1. Bonding modes.

X = I; types 1 and 2 for X = Br; and type 3 for X = Cl (scheme 1) [27]. For silver(I), there is only type 2 reported with Hbtsc-NH_2 for X = Br [20]. For R^1 = OH and R^2 = H, the salicylaldehyde thiosemicarbazone (H_2stsc-NH_2) behaved differently, forming type 1 compound with copper(I) chloride instead of type 3 formed by Hbtsc-NH_2; with copper(I) bromide and copper(I) iodide, both types 2 and 3 exist in the same crystal lattice (bond isomerism) [15]. For silver(I) chloride, H_2stsc-NH_2 formed type 3 compound and with silver(I) bromide exhibited bond isomerism similar to that shown by copper(I) bromide/iodide [15]. Among N^1-susbstituted thiosemicarbazones, salicylaldehyde N-methylthiosemicarbazone (H_2stsc-NHMe, R^2 = methyl) with copper(I) chloride formed type 1 compound (similar to that with H_2stsc-NH_2), and with copper(I) bromide and iodide, formed type 3 compounds and did not exhibit bond isomerism (unlike the behavior shown with H_2stsc-NH_2) [15]. Silver(I) chloride and bromide both have formed type 1 compounds with H_2stsc-NHMe, similar to that formed by copper(I) chloride.

Continuing to investigate the effect of substituents at C^2 and N^1 of thiosemicarbazones, in this article we describe coordination chemistry of copper(I) and silver(I) halides with salicylaldehyde N-ethylthiosemicarbazone (H_2stsc-NHEt).

2. Experimental

Copper(I) halides were prepared by reduction of $CuSO_4 \cdot 5H_2O$ using SO_2 in the presence of NaX (X = Cl, Br, and I) in distilled water. Silver(I) halides were prepared by the reaction of silver(I) nitrate in methanol with NaX (X = Cl, Br) [30]. The N-ethyl thiosemicarbazide, salicylaldehyde, and PPh_3 were procured from Aldrich Sigma Ltd. Salicylaldehyde N-ethylthiosemicarbazone was prepared by the condensation of salicylaldehyde with N^1-ethylthiosemicarbazide. Elemental analyses for C, H, and N were carried out using a thermoelectron FLASHEA1112 analyzer. The melting points

were determined with a Gallenkamp electrically heated apparatus. Infrared (IR) spectra of the ligand and complexes were recorded from 4000 cm^{-1} to 200 cm^{-1} (using KBr pellets) on FTIR-SHIMADZU 8400 Fourier Transform and Pye Unicam SP-3-300 spectrophotometers. ^{1}H NMR spectra of complexes were recorded in $CDCl_3$ with TMS as the internal reference on a AL-300 FT JEOL spectrometer operating at 300 MHz.

2.1. *Synthesis of [CuCl(η^1-S-H_2stsc-NHEt)(PPh_3)$_2$]·(0.33$CHCl_3$) (1)*

To a solution of copper(I) chloride (0.020 g, 0.20 mmol) in acetonitrile (6 mL) was added PPh_3 (0.106 g, 0.40 mmol). The solution was stirred for 2 h until cream colored precipitate formed. Acetonitrile was removed by decantation and chloroform was added to the precipitate followed by the addition of H_2stsc-NHEt (0.045 g, 0.20 mmol), and the contents were stirred for 5 min. After addition of methanol and refluxing for 5 min, a clear solution was obtained. On slow evaporation of solution at room temperature, yellow crystals of **1** formed. Yield: 72%; m.p. 174–178°C. Anal. Calcd for $C_{46.33}H_{43.33}Cl_2CuN_3OP_2S$: C, 62.71; H, 4.89; N, 4.74. Found: C, 62.41; H, 5.16; N, 4.42. Main IR peaks (KBr, cm^{-1}); ν(O–H), 3380(m); $\nu(N^1–H)$, 3240(b); $\nu(N^2–H)$, 3110(b); ν(C–H), 3000(s); ν(C=N) + ν(C=C), 1615, 1570(s); ν(C–N), 1035(b); $\nu(P–C_{Ph})$, 1110(m); ν(C=S), 965(b). ^{1}H NMR (δ, ppm, J, Hz, $CDCl_3$): 12.49 (s, N^2H); 9.59 (s, OH); 8.38 (s, C^2H); 7.30 (m, 32H; $C^{5,6}$H, Ph–P); 6.96 (m, $C^{7,8}$H); 3.63 (t, N^1CH_2); 1.22 (t, CH_3).

2.2. *Synthesis of [AgCl(η^1-S-H_2stsc-NHEt)(PPh_3)$_2$] (2)*

To AgCl (0.025 g, 0.17 mmol) suspended in acetonitrile (10 mL) was added H_2stsc-NHEt (0.038 g, 0.17 mmol). The contents were stirred for 24 h until precipitate formed. To the precipitate PPh_3 (0.090 g, 0.34 mmol) was added with stirring until a clear solution was obtained and the resulting solution was kept for crystallization. Yellow crystalline compound was formed. Crystals were grown from a mixture of CH_2Cl_2 and CH_3CN. Yield: 70%; m.p. 175–180°C. Anal. Calcd for $C_{46}H_{43}AgClN_3OP_2S$: C, 62.00; H, 4.83. Found: C, 62.60; H, 4.73. ^{1}H NMR (δ, ppm, J, Hz, $CDCl_3$) 12.20 (s, N^2H); 9.59 (s, OH); 8.61 (s, C^2H); 7.32 (m, 32H); $C^{5,6}$, Ph–P); 6.54 (s, N^1H); 6.94 (m, $C^{7,8}$H); 3.70 (t, N^1CH_2); 1.26(t, CH_3).

2.3. *Synthesis of [AgBr(η^1-S-H_2stsc-NHEt)(PPh_3)$_2$] (3)*

To AgBr (0.025 g, 0.13 mmol) suspended in acetonitrile (10 mL) was added H_2stscN-Et (0.029 g, 0.13 mmol). The solution was stirred for 24 h until white precipitate formed. To the precipitate PPh_3 (0.068 g, 0.26 mmol) was added and stirred until a clear solution was obtained. Slow evaporation of the filtrate containing about 5 mL of CH_2Cl_2 yielded white transparent crystals. Yield: 75%; m.p. 179–182°C. Anal. Calcd for $C_{46}H_{43}AgBrN_3OP_2S$: C, 59.00; H, 4.60; N, 4.49. Found: C, 59.53; H, 4.58; N, 4.77. ^{1}H NMR data (δ, ppm, J, Hz, $CDCl_3$): 11.42 (s, N^2H); 9.52 (s, OH); 8.57 (s, C^2H); 7.33 (m, 32H; $C^{5,6}$, Ph–P); 6.54 (s, N^1H); 6.94 (m, $C^{7,8}$H); 3.69 (t, N^1CH_2); 1.2 (t, CH_3).

2.4. *Synthesis of [CuBr(μ-S-H_2stsc-NHEt)(PPh_3)]$_2$·2$CHCl_3$ (4)*

To a solution of copper(I) bromide (0.033 g, 0.27 mmol) in acetonitrile (8–10 mL) was added PPh_3 (0.063 g, 0.23 mmol). The solution was stirred for 1.5 h and cream colored precipitate formed. Acetonitrile was removed by decantation and chloroform was added to the precipitate followed by the addition of H_2stsc-NHEt (0.054 g, 0.24 mmol); the contents were stirred for 5–10 min giving a clear solution. Slow evaporation of the solution at room temperature resulted in green crystals of **4**. Yield: 73%; m.p. 176–178°C. Anal. Calcd for $C_{58}H_{58}Br_2Cl_6Cu_2N_6O_2P_2S_2$: C, 46.50; H, 3.88. Found: C, 46.86; H, 4.07. Main IR peaks (KBr, cm^{-1}); ν(OH), 3350(m); $\nu(N^1H)$, 3280(b); $\nu(N^2H)$, 3080(m); ν(C–H), 2950(s); ν(C=N) + ν(C=C), 1610, 1570 (s); $\nu(P-C_{Ph})$, 1150(m); ν(C–N), 1030(b); ν(C=S), 950(b). ^{1}H NMR (δ, ppm, J, Hz, $CDCl_3$) 12.26(s, N^2H); 9.51(s, OH); 8.61(s, C^2H); 7.41(m, 32H; $C^{5,6}H$, Ph–P); 6.53(s, N^1H); 6.96 (m, $C^{7,8}H$); 3.70 (m, N^1CH_2); 1.56 (t,CH_3).

2.5. *Synthesis of [CuI(μ-S-H_2stsc-NHEt)(PPh_3)]$_2$·2CH_3CN (5)*

To a solution of copper(I) iodide (0.036 g, 0.19 mmol) in acetonitrile (8–10 mL) was added PPh_3 (0.048 g, 0.18 mmol). The solution was stirred for 1.5 h giving cream colored precipitate. Acetonitrile was removed by decantation and chloroform was added to the precipitate followed by the addition of H_2stsc-NHEt (0.044 g, 0.20 mmol); the contents were stirred for 5–10 min giving a clear solution. Slow evaporation of the solution at room temperature resulted in yellow crystals of **5**. Yield: 74%; m.p. 194–196°C. Anal. Calcd for $C_{60}H_{62}Cu_2I_2N_8O_2P_2S_2$: C, 50.21; H, 4.32; N, 7.81. Found: C, 50.47; H, 4.33; N, 8.01. Main IR peaks (KBr, cm^{-1}); ν(OH), 3380(m); $\nu(N^1H)$, 3340(b); $\nu(N^2H)$, 3125(m); ν(C–H), 3005(s); ν(C=N) + ν(C=C), 1635, 1585 (s); $\nu(P-C_{Ph})$, 1125(m); ν(C–N), 1055(b); ν(C=S), 970(b). ^{1}H NMR (δ, ppm, J, Hz, $CDCl_3$) 11.59(s, N^2H); 9.46(s, OH); 8.65(s, C^2H); 7.38(m, 32H; $C^{5,6}H$, Ph–P); 6.56(s, N^1H); 6.96 (m, $C^{7,8}H$); 3.69 (t, N^1CH_2); 1.57 (t, CH_3).

2.5.1. Ligand. IR bands (KBr pellets, cm^{-1}); ν(OH), 3695(s); $\nu(N^1H)$, 3400, 3360(s); $\nu(N^2H)$, 3170(w); ν(C–H), 3040(s); ν(C=N) + ν(C=C), 1615, 1555(b); ν(C–N), 1050(s); ν(C=S), 940(s). ^{1}H NMR data (δ, ppm, J, Hz, $CDCl_3$): 10.73 (s, OH), 9.68 (sb, N^2H), 8.18 (s, C^2H), 7.30 (m, $C^5H + C^6H$), 7.08 (sb, N^1H), 6.91 (m, $C^7H + C^8H$), 3.31 (m, CH_2), 1.28 (t, CH_3).

2.6. *Crystallography*

The single crystals of **1**–**5** were mounted on glass fibers and data were collected using a goniometer Xcalibur and Ruby (Gemini Cu) detector, each equipped with a graphite monochromator and Cu-Kα radiation (λ = 1.54184 Å) for **1**, and Mo-Kα radiation (λ = 0.71073 Å) for **2**–**5**. The unit cell dimensions and intensity data were measured at 110(2) (**1**), 123(2) (**3**–**5**), or 295(2) (**2**). The data were processed (data collection, refinement, and reduction) with *CrysAlisPro*. The structures were solved by direct methods using SHELXS-97 and refined by full-matrix least-squares based on F^2 using SHELXL-97. All non-hydrogen atoms were refined anisotropically. The crystallographic data are given in table 1.

Table 1. Crystal data for **1–5**.

Compound	**1**	**2**	**3**	**4**	**5**
Empirical formula	$C_{46.33}H_{43.33}Cl_2CuN_3OP_2S$	$C_{46}H_{43}ClAgN_3OP_2S$	$C_{46}H_{43}BrAgN_3OP_2S$	$C_{58}H_{58}Br_2Cl_6Cu_2N_6O_2P_2S_2$	$C_{60}H_{62}I_2Cu_2N_8O_2P_2S_2$
Formula weight	886.61	891.15	935.61	1496.76	1434.12
Temperature (K)	110(2)	295(2)	123(2)	123(2)	123(2)
Crystal system	Rhombohedral	Triclinic	Triclinic	Triclinic	Triclinic
Space group	*R*-3	*P*-1	*P*-1	*P*-1	*P*-1
Unit cell dimensions (Å, °)					
a	25.867(9)	10.6858(6)	10.6321(3)	10.7176(5)	10.4329(6)
b	25.867(9)	13.4561(8)	13.5059(3)	11.8812(4)	11.9911(6)
c	33.582(4)	15.6635(8)	15.2701(4)	13.9021(4)	13.6657(5)
α	90	77.077(5)	77.294(2)	95.071(3)	70.876(4)
β	90	79.773(5)	80.130(2)	108.069(3)	83.200(4)
γ	120	80.997(5)	83.121(2)	108.588(3)	66.647(5)
Volume (Å^3), *Z*	19460(10), 6	2144.2(2), 2	2099.67(9), 2	1560.35(10), 1	1482.81(14), 1
Calculated density (Mg m^{-3})	1.362	1.380	1.480	1.593	1.606
Absorption coefficient (mm^{-1})	3.302	0.694	1.596	2.384	1.932
F(000)	8268	916	952	756	720
Crystal size (mm^3)	0.28 × 0.17 × 0.08	0.44 × 0.39 × 0.23	0.37 × 0.24 × 0.19	0.44 × 0.41 × 0.16	0.44 × 0.21 × 0.15
θ range for data collection (°)	4.16–74.49	5.04–29.43	5.1054–32.6653	5.05–32.65	5.04–32.78
Reflections collected	15,595	22,931	28,479	21,029	19,253
Independent reflections	8339 [*R*(int) = 0.0786]	10,173 [*R*(int) = 0.0570]	13,816 [*R*(int) = 0.0543]	10,313 [*R*(int) = 0.0307]	9741 [*R*(int) = 0.0624]
Goodness-of-fit on F^2	1.058	0.897	0.977	0.926	1.023
R indices [$I > 2\sigma(I)$] (all data)	$R_1 = 0.0790$, $wR_2 = 0.2153$	$R_1 = 0.0566$, $wR_2 = 0.1532$	$R_1 = 0.0381$, $wR_2 = 0.1066$	$R_1 = 0.0353$, $wR_2 = 0.0768$	$R_1 = 0.0525$, $wR_2 = 0.1883$

3. Results and discussion

3.1. *Synthesis and spectroscopy*

Copper(I) chloride was first reacted with one mole of PPh_3 in acetonitrile and to the white precipitate suspended in chloroform was added one mole of H_2stsc-NHEt; however, no clear solution was formed. Thus use of two moles of PPh_3 instead of one was necessary for obtaining a clear solution. Copper(I) bromide and iodide were reacted with PPh_3 and H_2stsc-NHEt in 1 : 1 : 1 molar ratios in the same sequence and formed clear solutions. For silver, H_2stsc-NHEt was first reacted with silver(I) chloride or bromide in acetonitrile in 1 : 1 molar ratio and then addition of two moles of PPh_3 was necessary to get a clear solution. Slow evaporation of the solutions in each case gave crystals of $[CuCl(\eta^1\text{-S-}H_2\text{stsc-NHEt})(PPh_3)_2]$ (**1**), $[AgX(\eta^1\text{-S-}H_2\text{stsc-NHEt})(PPh_3)_2]$ (Cl, **2**; Br, **3**), and $[Cu_2X_2(\mu\text{-S-}H_2\text{stsc-NHEt})_2(PPh_3)_2]$ (X = Br, **4**; I, **5**). IR spectra show various bands due to ν(O–H), $\nu(N^1\text{–H})$, $\nu(N^2\text{–H})$, $\nu(C\text{–}H_{aryl})$, ν(C=S), $\nu(P\text{–}C_{Ph})$ and some other bands at positions different from the free ligand supporting that the thio-ligand coordinates to metal as a neutral ligand. Complexes **1**–**5** show ^{1}H NMR signals for N^2H, OH, C^2H, and N^1H protons at δ 11.59–12.49, 9.46–9.59, 8.38–8.65, and 6.53–6.56 ppm, respectively. The ethyl protons were also identified at δ 3.63–3.70(CH_2) and 1.2–1.56 ppm(CH_3). These NMR signals were at positions altered from those of the thio-ligand.

3.2. *Crystal and molecular structures*

The crystal data for **1**–**5** are given in table 1; table 2 contains important bond lengths and angles. Table 3 shows a comparison of analogous complexes with different bonding trends. Complex **1** crystallizes in rhombohedral crystal system with *R*-3 space group, while **2**–**5** crystallize in the triclinic crystal system with triclinic space group.

3.2.1. Molecular structures (1–5). In **1**, Cu^I is bonded to two PPh_3 at Cu–P bond distances, 2.2395(17) and 2.2578(17) Å, one sulfur of H_2stsc-NHEt and one Cl^- at 2.3567(17) and 2.4493(16) Å, respectively (figure 1). Cu−Cl distances are much less than the sum of ionic radii of Cu^+ and Cl^- (2.58 Å) [31]. Also, the Cu−P and Cu–S bond distances are close to other monomeric complexes with two Ph_3P ligands [15, 27, 32]. The C–S bond distance is 1.704(6) Å, significantly longer than the C=S double bond distance of 1.62 Å but shorter than a C–S single bond distance of 1.81 Å, suggesting partial double bond character in the C–S bond [33]. Angles around Cu are 99.04(6)–130.84(6)° with P–Cu–P bond angle being largest and P–Cu–Cl being smallest. With methyl substituent at N^1, the angles are 102.02(7)–123.68(7)° with P–Cu–P bond angle being largest and P–Cu–Cl being smallest [15]. Thus the angles around Cu vary with variation in substituents at N^1. The bonding pattern in **2** is similar to that of its N-methyl analog, $[AgCl(\eta^1\text{-S-}H_2\text{stsc-NHEt})(PPh_3)_2]$ [15]. There is marginal difference in Ag–P, Ag–S, and Ag–Cl distances of **2** in comparison to its N-methyl analog (cf. Ag–P, 2.4716(4), 2.4746(4); Ag–S, 2.5924(4) and 2.7192(4) Å) [15]. The angles around Ag are 98.17(4)–115.53(4)°,

Table 2. Selected bond lengths (Å) and angles (°) for **1–5**.

1			
Cu–P1	2.2395(17)	Cu–S	2.3567(17)
Cu–P2	2.2578(17)	Cu–Cl	2.4493(16)
S–C8	1.704(6)	P1–Cu–P2	130.84(6)
P1–Cu–S	110.48(6)	P2–Cu–Cl	100.09(6)
P2–Cu–S	102.91(6)	S–Cu–Cl	112.75(6)
P1–Cu–Cl	99.04(6)	C8–S–Cu	109.46(19)
2			
Ag–P1	2.4991(11)	Ag–S	2.6056(11)
Ag–P2	2.4736(10)	Ag–Cl	2.6591(12)
S–C1	1.690(5)	P1–Ag–P2	113.76(4)
P1–Ag–S	115.53(4)	P2–Ag–Cl	108.92(4)
P2–Ag–S	108.14(3)	S–Ag–Cl	98.17(4)
P1–Ag–Cl	111.12(4)	C1–S–Ag	102.50(15)
3			
Ag–P1	2.4599(6)	Ag–S	2.6082(6)
Ag–P2	2.4776(6)	Ag–Br	2.7206(3)
S–C8	1.700(2)	P1–Ag–P2	113.81(2)
P1–Ag–S	107.382(19)	P2–Ag–Br	114.171(16)
P2–Ag–S	115.03(2)	S–Ag–Br	98.686(16)
P1–Ag–Br	106.375(16)	C8–S–Ag	101.64(8)
4			
Cu–P	2.2426(6)	Cu–S	2.4654(5)
Cu–S	2.3711(5)	Cu–Br	2.4371(3)
S–C8	1.715(2)	Cu···Cu	3.134(1)
S–Cu–S	99.254(17)	P–Cu–S	106.20(2)
Cu–S–Cu	80.745(17)	P–Cu–S	115.918(19)
C8–S–Cu	112.67(7)	S–Cu–Br	114.988(16)
C8–S–Cu	104.80(6)	S–Cu–Br	103.859(15)
		P–Cu–Br	115.709(17)
5			
Cu–P	2.2632(10)	Cu–S	2.4404(10)
Cu–S	2.3789(12)	Cu–I	2.6350(5)
S–C8	1.726(4)	Cu···Cu	2.9704(9)
S–Cu–S	103.91(3	P–Cu–S	107.69(4)
Cu–S–Cu	76.09(3)	P–Cu–S	118.40(4)
C8–S–Cu	114.94(14)	S–Cu–I	117.12(3)
C8–S–Cu	102.53(13)	S–Cu–I	101.04(3)
		P–Cu–I	109.02(3)

Table 3. A comparison of bonding trends of **1–5** with previously reported complexes.

Metal salt	Hbtsc-NH_2 (R^1, R^2 = H, H)	H_2stsc-NH_2 (R^1, R^2 = OH, H)	H_2stsc-NHMe (R^1, R^2 = OH, Me)	H_2stsc-NHR^2 (R^1, R^2 = OH, Et)
CuCl	(μ-S), Type 3	(η^1-S), Type 1	(η^1-S), Type 1	(η^1-S), Type 1
CuBr	(η^1-S), Type 1 & (μ-Br), Type 2	(μ-Br) + (μ-S), Types 2 and 3 (Bond isomerism)	(μ-S), Type 3	(μ-S), Type 3
CuI	(η^1-S), Type 1	(μ-I) + (μ-S), Types 2 and 3 (Bond isomerism)	(μ-S), Type 3	(μ-S), Type 3
AgCl	–	(μ-S), Type 3	(η^1-S), Type 1	(η^1-S), Type 1
AgBr	(μ-Br), Type 2	(μ-Br) + (μ-S), Types 2 and 3 (Bond isomerism)	(η^1-S), Type 1	(η^1-S), Type 1
Reference	[20, 27]	[15]	[15]	This work

See scheme 1 for details of ligands and types of complexes. Type 1 is mononuclear, type 2 is halogen bridged dinuclear, type 3 is sulfur-bridged dinuclear. Bond isomerism refers to the existence of both types 2 and 3 in the same lattice.

different from its methyl analog (cf. 100.634(13)–125.395(14)°) [15]. The P–Ag–P in **2** is much smaller (113.76(4)°) than found in its methyl analog, i.e., 122.859(14)°. The bonding pattern of **3** is similar to that of **2** with P–Ag–P angle of 113.81(2)° (figures 2 and 3).

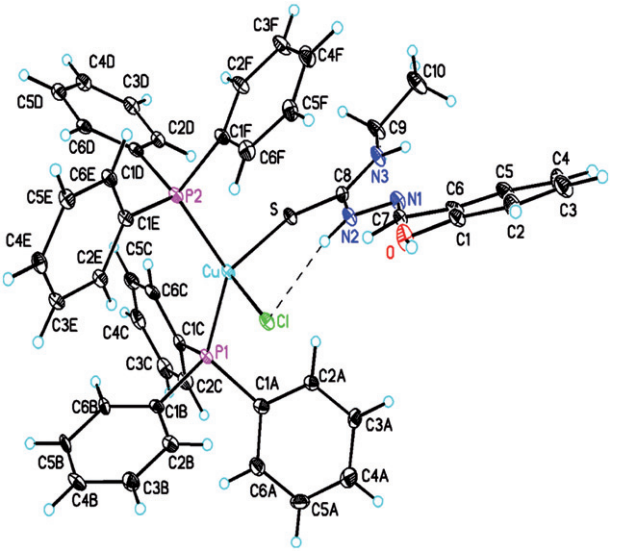

Figure 1. Molecular structure of $[CuCl(\eta^1\text{-S-H}_2\text{stsc-NHEt})(PPh_3)_2]\cdot 0.33CHCl_3$ (**1**).

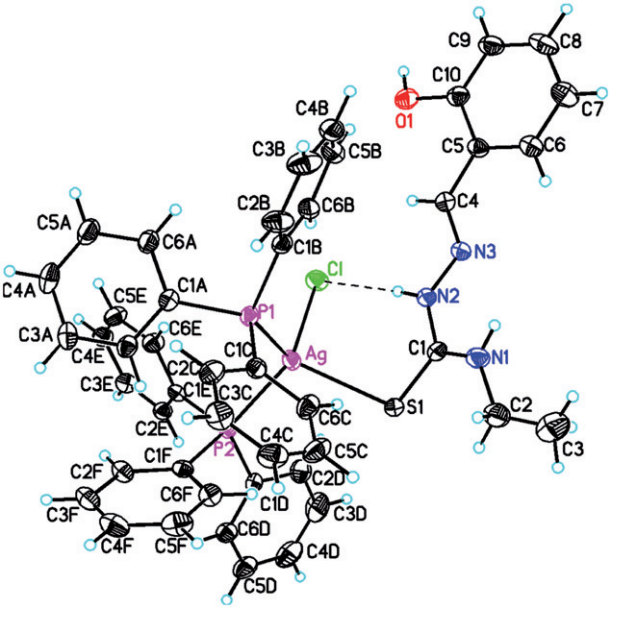

Figure 2. Molecular structure of $[AgCl(\eta^1\text{-S-H}_2\text{stsc-NHEt})(PPh_3)_2]$ (**2**).

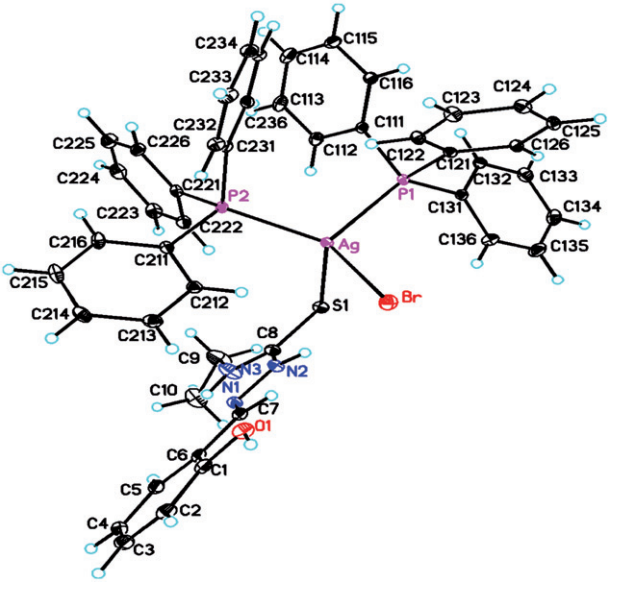

Figure 3. Molecular structure of $[AgBr(\eta^1\text{-S-}H_2stsc\text{-}NHEt)(PPh_3)_2]$ (**3**).

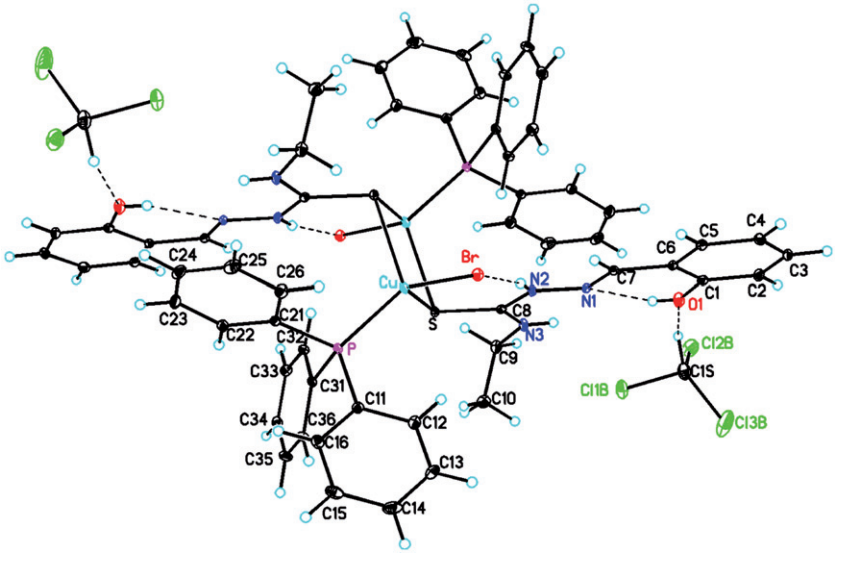

Figure 4. Molecular structure of $[CuBr(\mu\text{-S-}H_2stsc\text{-}NHEt)(PPh_3)]_2 \cdot 2CHCl_3$ (**4**).

In **4**, each Cu is bonded to one terminal Br, two bridging S, and one PPh_3, thus acquiring four-coordination (figure 4). The central core $Cu(\mu\text{-}S)_2Cu$ has unequal Cu–S distances, 2.3711(5) and 2.4654(5) Å, forming a parallelogram. The Cu–P and Cu–Br bond distances are 2.2426(6) and 2.4371(3) Å. Angles around each copper reveal a

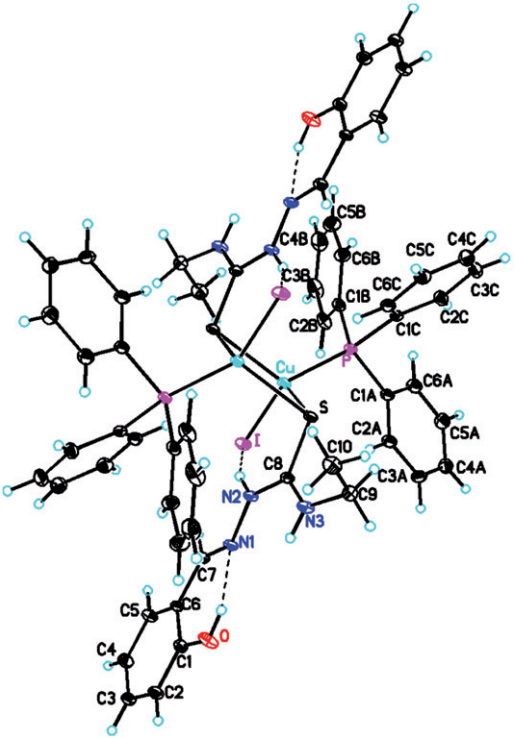

Figure 5. Molecular structure of $[CuI(\mu\text{-S-}H_2stsc\text{-}NHEt)(PPh_3)]_2 \cdot 2CH_3CN$ (**5**).

distorted tetrahedral geometry (80.745(17)–115.918(19))°. Bond parameters of **5** are similar to **4** (figure 5). The Cu···Cu separation in **5** (2.9704(9) Å) is smaller than in **4** (3.134(1) Å). As expected the C–S bond distances are longer in **4** and **5** due to sulfur bridging, intermediate in **1** and shortest in **2** and **3**. Further, angles at Cu and S of the central cores are much different due to the presence of bulkier iodide in **5**.

3.3. *Packing interactions*

Complexes **1**–**5** exhibit different types of intra- and intermolecular hydrogen bonds due to the absence or presence of solvent in the crystal lattice (table 4). In mono- and dinuclear complexes, the halides form intramolecular hydrogen bonds with hydrazinic hydrogen at N^2 (**1**, Cl···N^2, 3.160; **2**, Cl···N^2, 3.290; **3**, Br···N^2, 3.424; **4**, Br···N^2, 3.316; **5**, I···N^2, 3.607; Å). In dinuclear complexes, 2-hydroxy is engaged in intramolecular hydrogen-bonding with azomethine nitrogen (HO···N^3, 2.092, **4**; 1.974, **5**; Å), while in mononuclear (**1**–**3**) it is engaged in intermolecular hydrogen-bonding with halide (O–H···Cl, 2.291, **1**; 2.258 **2**, O–H···Br, 2.389 **3**; Å).

Table 4. Hydrogen bonds for **1–5** (Å and °).

D–H···A	*d*(D–H)	*d*(H···A)	*d*(D···A)	∠(DHA)
1				
N(2)–H(2)···Cl	0.88	2.29	3.159(5)	170.3
N(3)–H(3B)···Cl(1)	0.88	2.96	3.722(6)	145.5
O–H(0A)···Cl	0.84	2.29	3.131(4)	177.2
C(10)–H(10C)···Cl(1)	0.98	2.841	3.489	124.33
C(3A)–H(3AA)···C(6B)	0.947	2.872	3.745	153.71
C(6A)–H(6AA)···C(3A)	0.949	2.701	3.638	169.67
C(10)–H(10A)···C(6D)	0.980	2.845	3.585	132.86
C(10)–H(10A)···C(5D)	0.980	2.778	3.511	132.04
C(4A)–H(4AA)···C(4E)	0.950	2.708	3.613	159.53
C(4A)–H(4AA)···C(5E)	0.950	2.868	3.570	122.33
2				
O(1)–H(1)···Cl	0.82	2.26	3.063(3)	166.9
N(2)–H(2C)···Cl	0.86	2.43	3.290(4)	176.1
C(6D)–H(6DA)···C(3E)	0.93	2.829	3.668	150.67
C(2C)–H(2CA)···C(6)	0.93	2.837	3.395	139.37
3				
O(1)–H(1A)···Br	0.84	2.39	3.1948(18)	161.0
N(2)–H(2B)···Br	0.84	2.55	3.424(2)	173.1
C(114)–H(11C)···S(1)	0.95	2.993	3.873	154.78
C(3)–H(3A)···C(124)	0.95	2.895	3.518	124.29
C(226)–H(22E)···C(5)	0.95	2.762	3.473	132.19
4				
O(1)–H(10)···N(1)	0.68(3)	2.09(3)	2.691(2)	148(3)
N(2)–H(2N)···Br	0.75(2)	2.58(2)	3.3154(18)	171(2)
C(15)–H(15A)···O(1)	1.000	2.478	3.180	126.92
C(23)–H(23A)···Cl(2A)	0.958	2.723	3.555	146.67
5				
O–H(0)···N(1)	0.84	1.97	2.708(4)	145.5
N(2)–H(2B)···I	0.88	2.81	3.607(4)	151.1
N(3)–H(3B)···N(1S)	0.88	2.41	3.116(6)	137.4
C(3B)–H(3BA)···C(3A)	0.95	2.682	3.550	152.19
C(2S)–H(2S1)···O	0.979	2.708	3.284	1118.00

In **1**, one independent molecule is connected with adjacent molecules through C−H···π(ph) (2.701, 2.872 Å) interactions between phenyl rings of PPh_3 forming a dinuclear unit. This unit has no direct interaction with similar units, however, these units interact indirectly *via* $CHCl_3$ present in the lattice {$(N^1)H_2CH\cdots Cl$, 2.841 Å} and form a zig-zag 1-D chain. This chain is connected with similar adjacent chains through O–H···Cl, 2.291 and $(N^1)H_2CH\cdots Cl$, 2.841 Å interactions forming a 2-D sheet (figure 6). In **2**, there is no solvent present in the lattice. Interactions between phenyls of PPh_3 of adjacent molecules {C–H···π(ph), 2.829 Å} form a dinuclear unit. Two dinuclear units are connected through interaction between hydroxyl and chloride (O–H···Cl, 2.258 Å). Repetition of these interactions led to formation of 1-D chains. The 2-D sheet is formed *via* C–H···π(ph), 2.837 and $(C^2{=}N)\pi\cdots\pi$(ph), 3.367 Å interactions (figure 7).

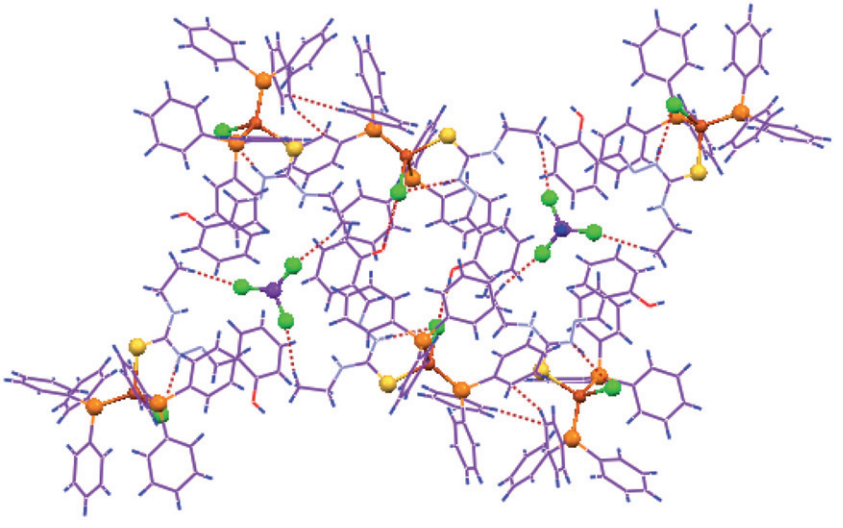

Figure 6. Packing interactions in **1**.

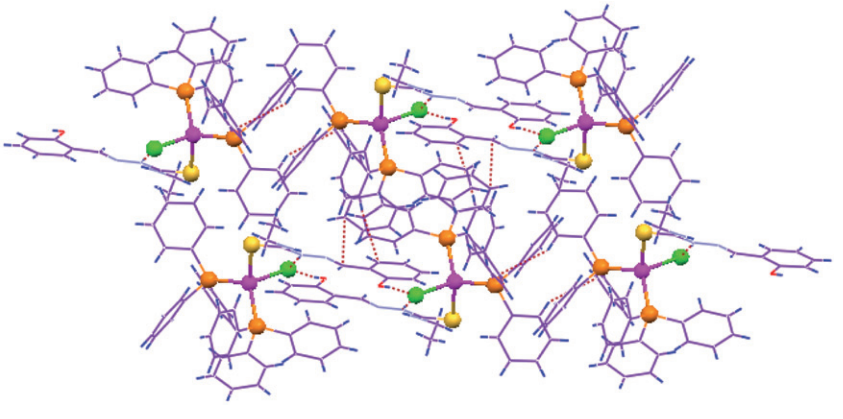

Figure 7. Packing interactions in **2**.

In **3**, a 1-D chain is formed through C–H $\cdots$ π(ph), 2.762 and C–H $\cdots$ π(S=C), 2.993 Å interactions. Interactions between adjacent 1-D chains {O–H $\cdots$ Br, 2.389 and C–H $\cdots$ π(ph), 2.895 Å} form a 2-D sheet (figure 8). In **4**, one dinuclear unit is connected to the adjacent dinuclear unit through (N=N)π $\cdots$ π(ph), 3.248; (ph)π $\cdots$ π(ph), 3.390; and (C^2=N)π $\cdots$ π(ph), 3.275 Å interactions, resulting in formation of 1-D chains. There is no direct contact between two adjacent 1-D chains but these are connected through $CHCl_3$ present in the lattice {H–O $\cdots$ H–CCl_3, 2.478; C–H $\cdots$ Cl–$CHCl_2$, 2.723 Å} forming 2-D sheets (figure 9). In **5**, 1-D chain is formed by (ph)π $\cdots$ π(ph), 3.292 Å interaction of PPh_3 of adjacent molecules. A 2-D sheet is formed either through interactions between adjacent 1-D chains {(C=S)π $\cdots$ π(ph),

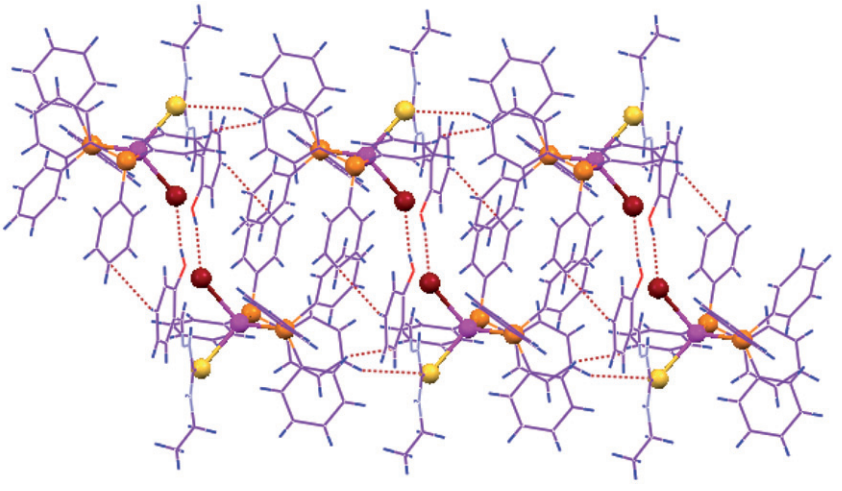

Figure 8. Packing interactions in **3**.

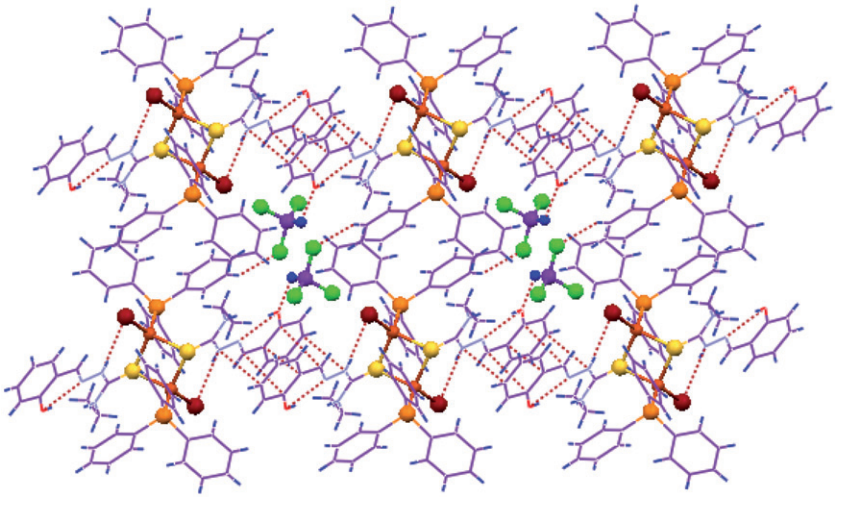

Figure 9. Packing interactions in **4**.

3.378; (C^2=N)$\pi\cdots\pi$, 3.367 Å} or through CH_3CN present in the lattice {H–O$\cdots$H–CH_2CN, 2.708; N^1–H$\cdots$N–CCH_3, 2.410 Å} (figure 10).

4. Conclusion

Coordinating properties of H_2stsc-NHMe and H_2stsc-NHEt are similar with CuCl, AgCl, and AgBr forming η^1-S bonded tetrahedral complexes, while with CuBr and CuI,

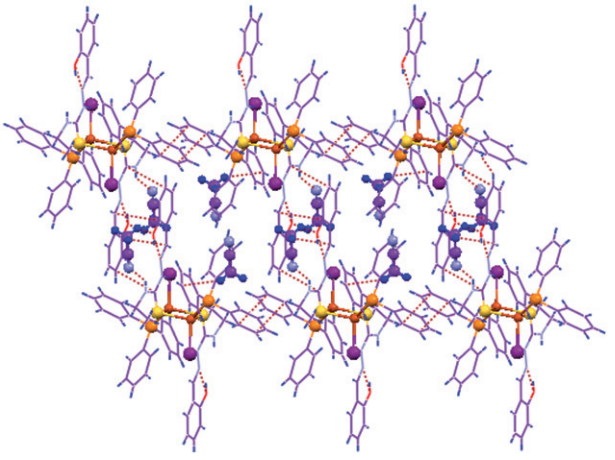

Figure 10. Packing interactions in **5**.

they formed μ-S bridged dinuclear complexes. H_2stsc-NH_2 forms η^1-S bonded tetrahedral complex with CuCl, μ-S bridged dinuclear complex with AgCl and bond isomerism with CuBr, AgBr, and CuI having μ-X and μ-S bridged molecules in the same unit. The absence of –OH substituent as in Hbtsc-NH_2 showed more random behavior: μ-S bridged with CuCl, η^1-S bonded and μ-Br bridged dimer with CuBr and η^1-S bonded with CuI.

Supplementary material

Full details have been deposited with the Cambridge Crystallographic Data Centre, CCDC for **1**–**5** are 858597–858601. Copies of this information can be obtained free of charge from The Director, CCDC, 12 Union Road, Cambridge CB2 1EZ, UK (Fax: 44-1223-336-033; E-mail: deposit@ccdc.cam.ac.uk; or http://www.ccdc.cam.ac.uk).

Acknowledgments

Financial support from CSIR, New Delhi (Scheme No. 01(1993)/05/EMR II) is gratefully acknowledged. JPJ acknowledges the NSF–MRI program (Grant No. CHE-1039027) for funds to purchase the X-ray diffractometer.

References

[1] T.S. Lobana, R. Sharma, G. Bawa, S. Khanna. *Coord. Chem. Rev.*, **253**, 977 (2009).
[2] T.S. Lobana, G. Bawa, A. Castineiras, R.J. Butcher, M. Zeller. *Organometallics*, **27**, 175 (2008).

[3] T.S. Lobana, G. Bawa, G. Hundal, M. Zeller. *Z. Anorg. Allg. Chem.*, **634**, 931 (2008).
[4] J. Garcia-Tojal, J.L. Pizarro, A. Garcia-Orad, A.R. Perez-Sanz, M. Ugalde, A.A. Diaz, J.L. Serra, M.I. Arriortua, T. Rojo. *J. Inorg. Biochem.*, **86**, 627 (2001).
[5] M.B. Ferrari, F. Bisceglie, G. Pelosi, P. Tarasconi, R. Albertini, A. Bonati, P. Lunghi, S. Pinelli. *J. Inorg. Biochem.*, **83**, 169 (2001).
[6] M.B. Ferrari, F. Bisceglie, G. Pelosi, P. Tarasconi, A. Albertini, P.P. Dall'Aglio, S. Pinelli, A. Bergamo, G. Sava. *J. Inorg. Biochem.*, **98**, 301 (2004).
[7] M.A. Ali, A.H. Mirza, A.M.S. Hossain, M. Nazimuddin. *Polyhedron*, **20**, 1045 (2001).
[8] M. Joseph, M. Kuriakose, M.R.P. Kurup, E. Suresh, A. Kishore, S.G. Bhat. *Polyhedron*, **25**, 61 (2006).
[9] T.S. Lobana, R. Sharma, A. Castineiras, R.J. Butcher. *Z. Anorg. Allg. Chem.*, **636**, 2698 (2010).
[10] T.S. Lobana, P. Kumari, R. Sharma, A. Castineiras, R.J. Butcher, T. Akitsu, Y. Aritake. *Dalton Trans.*, **40**, 3219 (2011).
[11] T.S. Lobana, S. Khanna, A. Castineiras, G. Hundal. *Z. Anorg. Allg. Chem.*, **636**, 454 (2010).
[12] T.S. Lobana, S. Khanna, G. Hundal, R.J. Butcher, A. Castineiras. *Polyhedron*, **28**, 3899 (2009).
[13] T.S. Lobana, R. Sharma. *Z. Anorg. Allg. Chem.*, **635**, 2150 (2009).
[14] T.S. Lobana, R. Sharma, A. Castineiras, G. Hundal, R.J. Butcher. *Inorg. Chim. Acta*, **362**, 3547 (2009).
[15] T.S. Lobana, S. Khanna, P. Kaur, B. Thakur, S. Attri, G. Hundal, R.J. Butcher. *Polyhedron*, **28**, 1538 (2009).
[16] T.S. Lobana, R. Sharma, R.J. Butcher. *Polyhedron*, **28**, 1103 (2009).
[17] T.S. Lobana, P. Kumari, A. Castineiras, R.J. Butcher. *J. Coord. Chem.*, **62**, 754 (2009).
[18] T.S. Lobana, R. Sharma, R. Sharma. *J. Coord. Chem.*, **62**, 1468 (2009).
[19] T.S. Lobana, S. Khanna, G. Hundal, B.-J. Liaw, C.W. Liu. *Polyhedron*, **27**, 2251 (2008).
[20] T.S. Lobana, S. Khanna, R. Sharma, G. Hundal, R. Sultana, M. Chaudhary, R.J. Butcher. *Cryst. Growth Des.*, **8**, 1203 (2008).
[21] T.S. Lobana, P. Kumari, R.J. Butcher. *Inorg. Chem. Commun.*, **11**, 11 (2008).
[22] T.S. Lobana, S. Khanna, A. Castineiras. *Inorg. Chem. Commun.*, **10**, 1307 (2007).
[23] T.S. Lobana, S. Khanna, R.J. Butcher. *Z. Anorg. Allg. Chem.*, **633**, 1820 (2007).
[24] T.S. Lobana, S. Khanna, R.J. Butcher, A.D. Hunter, M. Zeller. *Inorg Chem.*, **46**, 5826 (2007).
[25] T.S. Lobana, Rekha, A.P.S. Pannu, G. Hundal, R.J. Butcher, A. Castineiras. *Polyhedron*, **26**, 2621 (2007).
[26] T.S. Lobana, S. Khanna, R.J. Butcher, A.D. Hunter, M. Zeller. *Polyhedron*, **25**, 2755 (2006).
[27] T.S. Lobana, Rekha, R.J. Butcher, A. Castineiras, E. Bermejo, P.V. Bharatam. *Inorg. Chem.*, **45**, 1535 (2006).
[28] T.S. Lobana, Rekha, B.S. Sidhu, A. Castineiras, E. Bermejo, T. Nishioka. *J. Coord. Chem.*, **58**, 803 (2005).
[29] T.S. Lobana, Rekha, R.J. Butcher. *Trans. Met. Chem.*, **29**, 291 (2004).
[30] G. Brauer. *Handbook of Preparative Chemistry*, Vol. 2, 2nd Edn, Vol. 2, Academic Press, New York (1965).
[31] J.E. Huheey, E.A. Keiter, R.L. Keiter. *Inorganic Chemistry: Principals of Structure and Reactivity*, 4th Edn, Harper Collins College Publishers, New York (1993).
[32] T.S. Lobana, Rekha, B.S. Sidhu, A. Castineiras, E. Bermejo, T. Nishioka. *J. Coord. Chem.*, 58 (2005), and references therein.
[33] L. Pauling. *The Nature of the Chemical Bond*, 3rd Edn, Cornell University Press, New York (1960).